

Investigating the optimality of ancilla-assisted linear optical Bell measurements

Andrea Olivo^{1,2,*} and Frédéric Grosshans^{2,†}

¹*Inria, Paris, France*

²*Laboratoire Aimé Cotton, CNRS, Université Paris-Sud,
ENS Cachan, Université Paris-Saclay, 91405 Orsay Cedex, France*

(Dated: September 5, 2018)

In the last decade Grice [1] and Ewert and van Loock [2] found linear optical networks achieving near-unit efficiency unambiguous Bell state discrimination, when fed with increasingly complex ancillary states. However, except for the vacuum ancilla case [3], the optimality of these schemes is unknown. Here, the optimality of these networks is investigated through analytical and numerical means. We show an analytical upper bound to the success probability for interferometers that preserve the polarization of the input photons, saturated by both Grice’s and Ewert-van Loock’s strategies. Furthermore, such an upper bound links the complexity of their ancilla states with the scaling of their performance. We also show a computer-aided approach to the optimization of such measurement schemes for generic interferometers, by simulating an optical network supplied with various kinds of ancillary input states. We numerically confirm the optimality of known small schemes. We use both methods to investigate other ancilla states, some of them never studied before.

I. INTRODUCTION

Due to its experimental and theoretical simplicity, linear quantum optics has proved to be a promising route for the early implementation of important quantum communication protocols [4]—including quantum teleportation [5–7], dense coding [8, 9] and entanglement swapping [10, 11]. An essential step in these protocols is the *Bell measurement* (BM), a projective measurement onto a basis of two-qubit maximally entangled states, the Bell states. In order to enable the common scenario where losses can be tolerated but not errors, in the following we will be concerned with *unambiguous* BM, *i.e.* a measurement whose outcome is never wrong, but is sometimes inconclusive.

Lütkenhaus *et al.* [12] showed long ago the impossibility of a linear optical perfect Bell measurement for dual-rail photonic qubits. In a following result, Calsamiglia and Lütkenhaus bound the success probability $\mathcal{P}_{\text{succ}}$ of the no-ancilla case to 50% [3], thus proving the optimality of the already known Braunstein–Mann scheme [4]. Recently, Grice [1], followed by Ewert and van Loock [2] showed how to overcome this bound by supplying the network with ancillary states. They showed how to attain a success probability of $\mathcal{P}_{\text{succ}} = 3/4$ with reasonable ancillary states, and how to increase this probability to values arbitrarily close to 1, by using increasingly complex and entangled ancillæ. Other ways around the 50% barrier include feed-forward techniques from linear optical quantum computation [13, 14], squeezing operations [15], Kerr nonlinearities [16], entangled coherent states, hybrid entanglement [6, 17] or encoded qubits [18]. While some of the above techniques may in principle be used to realize a perfect BM, each one has its own disadvantages and present different experimental challenges in

their implementation. For linear optics the difficulties are concentrated in the preparation of complex ancillary states; this is partly compensated by the simplicity of interferometers.

Our main motivation in this work is to investigate the optimality of ancilla-assisted linear optical schemes: what is the highest possible $\mathcal{P}_{\text{succ}}$ for a given ancilla? Which are the “simplest” states to achieve a given value for $\mathcal{P}_{\text{succ}}$? Very recently, and independently from us, Smith and Kaplan [19] tackled a similar problem, optimizing the mutual information of a Bell measurement using single photon ancillæ.

In Section II, we first present an analytical upper bound to the success probability of ancilla-assisted BM for polarization-preserving interferometers. Specifically, this bound is saturated by the Grice scheme [1]. In Section III, we expose a linear optical network optimizer based on symbolic and numerical computations, built in order to maximize the success probability of unambiguous BM for a given ancillary state and to argue about its optimality. This program is available as supplementary material to this article [20]. In Section IV, we discuss the results obtained with the two approaches above with different kinds of ancillæ and compare them to previously known results [1–4, 19]. To our knowledge, some ancillæ studied here were never employed for this task. We also discuss some of the hidden symmetries of the problem at hand, some of which we exploit in order to lessen the amount of computation needed. Finally, we conclude this work in Section V.

II. ANALYTICAL UPPER BOUND FOR POLARIZATION-PRESERVING INTERFEROMETERS

A desirable goal is to find an unambiguous Bell measurement using linear optics with the best possible success probability $\mathcal{P}_{\text{succ}}$ and the simplest possible ancillary state.

* andrea.olivo@u-psud.fr

† frederic.grosshans@u-psud.fr

In this section, we present an analytical upper bound for the success probability $\mathcal{P}_{\text{succ}}$ of such unambiguous discrimination schemes using ancillary states and polarization preserving linear optics. This restriction to polarization preserving interferometers—*i.e.* networks described by a block-diagonal unitary $U = \text{diag}(U_h, U_v)$, with U_h (resp. U_v) acting on the horizontally (resp. vertically) polarized modes—is not motivated by experimental realities but is an artificial consequence of the proof technique. Specifically, this restriction will not be enforced in the computer aided optimization of Section III. However, the previously known schemes [1, 2, 4] are all polarization independent, *i.e.* polarization preserving with $U_h = U_v$, so this restriction still allows to achieve non trivial discrimination. The common polarization independence of these schemes was motivated by the symmetry of the Bell states set. We conjecture that the optimal interferometer presents the same symmetry, and is polarization independent, except for an initial preprocessing step of the ancillæ, as for the single-photon schemes of [2].

We present this polarization preserving upper bound for a generic ancilla in Section II A, and bound it itself by a simple photon number dependent expression in Section II B.

A. Generic upper bound

The ability of an interferometer to perform a BM is its ability to discriminate between the four Bell states when they are supplied as its input, each with equal probability 1/4. We consider, *w.l.o.g.*, a pure k -photon additional resource state $|\Upsilon\rangle = \sum_{\lambda=0}^k v_\lambda |\Upsilon, \lambda\rangle$, where $|\Upsilon, \lambda\rangle$ is a pure state with λ photons polarized horizontally and $k - \lambda$ photons polarized vertically. Since our interferometer is polarization preserving, the total number of horizontally (or vertically) polarized photons is unchanged, and this number can be easily deduced from the observed detection event. Therefore, the measurement would be the same if one had performed a projective measurement of these polarized photon numbers on the global input state, before feeding the projected state into the interferometer.

Let us rewrite the input state according to this projection:

$$\begin{aligned} |\Psi^\pm\rangle |\Upsilon\rangle &= \sum_{\lambda=1}^{k+1} \frac{v_{\lambda-1}}{\sqrt{2}} (|HV\rangle \pm |VH\rangle) |\Upsilon, \lambda-1\rangle \\ |\Phi^\pm\rangle |\Upsilon\rangle &= \sum_{\lambda=0}^{k+2} \frac{v_{\lambda-2}}{\sqrt{2}} |HH\rangle |\Upsilon, \lambda-2\rangle \pm \frac{v_\lambda}{\sqrt{2}} |VV\rangle |\Upsilon, \lambda\rangle, \end{aligned} \quad (1)$$

where we have set $v_\lambda = 0$ for $\lambda < 0$ and $\lambda > k$, in order to include the edge cases in the formula. Each term of the above sums corresponds to a term with λ horizontally polarized photons.

To obtain an upper bound, we assume the measurement to be perfect after the projection onto the state with λ

horizontally polarized photons and $(k+2) - \lambda$ vertically polarized ones, forgetting about the linear optics restriction. One can easily see in the above equations that, for each λ , the term corresponding to the states $|\Psi^+\rangle$, $|\Psi^-\rangle$, and $|\Phi^\pm\rangle$ are in three orthogonal subspaces, with the only possible remaining ambiguity being between the $|\Phi^+\rangle$ and $|\Phi^-\rangle$ states. Let us now look at the distinguishability of those states.

For an arbitrary ancillary state, the unambiguous discrimination has to be performed between the following unnormalized states:

$$|\Lambda^\pm\rangle = \frac{v_{\lambda-2}}{\sqrt{2}} |HH\rangle |\Upsilon, \lambda-2\rangle \pm \frac{v_\lambda}{\sqrt{2}} |VV\rangle |\Upsilon, \lambda\rangle.$$

Unambiguous discrimination of such a pair of pure states is possible with an optimal success probability [21–23] of $\|\Lambda\| - |\langle \Lambda^+ | \Lambda^- \rangle|$, with $\|\Lambda\| = \langle \Lambda^+ | \Lambda^+ \rangle = \langle \Lambda^- | \Lambda^- \rangle$. This optimal success probability is an upper bound to what is achievable with linear optics and photon counting, leading to

$$\mathcal{P}_{\text{succ}, \lambda} \leq 2 \min\left(\frac{1}{2} |v_{\lambda-2}|^2, \frac{1}{2} |v_\lambda|^2\right).$$

The total success probability—assuming an equal input probability of 1/4 for each Bell state, and perfect discrimination of $|\Psi^\pm\rangle$ —is then

$$\begin{aligned} \mathcal{P}_{\text{succ}} &\leq \frac{1}{2} + \frac{1}{2} \sum_{\lambda=0}^{k+2} \min\left(|v_{\lambda-2}|^2, |v_\lambda|^2\right) \\ &= \frac{1}{2} + \frac{1}{2} \sum_{\lambda \text{ even}} \min\left(|v_{\lambda-2}|^2, |v_\lambda|^2\right) \\ &\quad + \frac{1}{2} \sum_{\lambda \text{ odd}} \min\left(|v_{\lambda-2}|^2, |v_\lambda|^2\right). \end{aligned}$$

Since the minimum is taken every two value of λ , even and odd indices have to be considered separately. It is then easy to notice that, among even (resp. odd) values of λ , all values of $|v_\lambda|^2$ are counted once except the local maxima, which are omitted, and the local minima, which are counted twice, leading to

$$\begin{aligned} \mathcal{P}_{\text{succ}} &\leq 1 - \frac{1}{2} \sum_{\substack{\lambda \text{ even} \\ |v_\lambda|^2 \text{ loc max}}} |v_\lambda|^2 + \frac{1}{2} \sum_{\substack{\lambda \text{ even} \\ |v_\lambda|^2 \text{ loc min}}} |v_\lambda|^2 \\ &\quad - \frac{1}{2} \sum_{\substack{\lambda \text{ odd} \\ |v_\lambda|^2 \text{ loc max}}} |v_\lambda|^2 + \frac{1}{2} \sum_{\substack{\lambda \text{ odd} \\ |v_\lambda|^2 \text{ loc min}}} |v_\lambda|^2. \end{aligned} \quad (2)$$

This bound can then be simplified to the following looser bound on the failure probability

$$\mathcal{P}_{\text{fail}} \geq \frac{1}{2} \left(\max_{\lambda \text{ even}} (|v_\lambda|^2) + \max_{\lambda \text{ odd}} (|v_\lambda|^2) \right), \quad (3)$$

the latter being equivalent to (2) iff $|v_\lambda|^2$ has a single local maximum over even values of λ and a single local maximum over odd values of λ .

In Section IV, we will compute this bound for different ancillary states $|\Upsilon\rangle$. But for now, we can already use the above equations to compute a bound depending only on $|\Upsilon\rangle$'s photon number k .

B. Photon-number based upper bound

Let us now work out a bound that is independent of the specific form of $|\Upsilon\rangle$. If the number of photons k in the ancilla is odd, there are $\frac{k+1}{2}$ possible odd values for λ for which $v_\lambda \neq 0$, and as many even values. Eq. (2) then leads to the bound

$$\mathcal{P}_{k \text{ odd}}^{\text{fail}} \geq \frac{1}{k+1},$$

which can only be achieved by ancillary states where all even values of λ are equiprobable, and all odd values of λ are equiprobable. Similarly, if k is even, there are $\frac{k}{2}$ possible odd values for λ such that $v_\lambda \neq 0$, and $\frac{k}{2} + 1$ even ones. This leads to the bound

$$\mathcal{P}_{k \text{ even}}^{\text{fail}} \geq \frac{1}{k+2},$$

which can only be achieved by ancillary states where all values of λ for which $v_\lambda \neq 0$ are even and equiprobable.

Both limits above can be expressed by the formula

$$\mathcal{P}_{\text{fail}} \geq \frac{1}{\lceil k+1 \rceil_{\text{even}}}, \quad (4)$$

where $\lceil \cdot \rceil_{\text{even}}$ is the smallest even integer greater or equal to its argument. For the trivial case $k = 0$, this result is a special case of the Calsamiglia–Lütkenhaus theorem [3]. For $k = 1$, we find that a single extra photon does not help, at least with a polarization preserving interferometer.

A non-trivial example of state achieving the limit for even k is the $\{2^{N+1} - 2\}$ -photon ancillary state $|\Upsilon_1\rangle_G \cdots |\Upsilon_N\rangle_G$ defined by Grice in [1]. Note that, except for the 2-photon state $|\Upsilon_1\rangle_G = |\Phi^+\rangle$, the Grice scheme needs to use GHZ-like states [24] of up to 2^N dual-rail qubits. The $|\Upsilon_n\rangle_{\text{EVL}}$ states defined Ewert and van Loock in [2] can be written in the same form of the $|\Upsilon_n\rangle_G$ states of [1] with respect to the distribution of horizontally polarized photons; however, at variance with them, in order to attain the same $\mathcal{P}_{\text{succ}}$ two copies of each one are required. The photon-number dependent upper bound (4) is therefore not tight for them, even if the generic bound (3) is. However, the schemes by Ewert and van Loock start by independently interfering each of the output of an initial 50:50 beamsplitter with half of the ancillary state. This additional restriction changes the photon dependent bound, which is then achieved by the Ewert–van Loock schemes.

III. LINEAR OPTICAL NETWORK OPTIMIZER

We present here our linear optical network optimizer, a program looking for the optical network maximizing $\mathcal{P}_{\text{succ}}$ for a given ancillary state. We first restate our problem in terms of second quantization in Section III A before detailing our approach, which can be divided into

two parts. As explained in Section III B, for each ancilla we want to analyze, and for each input Bell state, we generate a symbolic expression for the probability amplitudes of all output events in terms of U . Those functions, along with their gradient with respect to the U entries, are heuristically optimized in order to reduce the number of operations needed. The optimized functions are then translated into a low-level language and compiled. Then, as exposed in Section III C, a constrained numerical optimization using a nonlinear method is performed. Due to the heavy non-smooth character of $\mathcal{P}_{\text{succ}}$, we construct a meaningful figure of merit, function of the previously obtained probability amplitudes.

While this can seem at first glance an overkill *brute-force* approach, both steps present important symmetries that we can exploit, gaining up to two orders of magnitude in computation time in some cases, and reducing function complexity.

A. Polynomial representation of the network

We can represent the input (output) state to a n -modes linear optical network through a polynomial in the input (output) modes creation operators [25]

$$\begin{aligned} |\psi_{\text{in}}\rangle &= P_{\text{in}}(a_1^\dagger, \dots, a_n^\dagger) |0\rangle, \\ |\psi_{\text{out}}\rangle &= P_{\text{out}}(c_1^\dagger, \dots, c_n^\dagger) |0\rangle. \end{aligned}$$

The effect of the network can be represented by a unitary transformation $U := (u_{ij})$ connecting the input and the output modes:

$$a_i^\dagger = \sum_{j=1}^n u_{ij} c_j^\dagger. \quad (5)$$

Notice that this only implements a subset of all the transformations of the modes allowed by quantum mechanics, namely photon interferences.

At variance with the previous section, we represent dual rail encoding with distinct spatial modes instead of orthogonal polarization modes [14]. The Bell states are represented by:

$$|\Phi^\pm\rangle = \frac{1}{\sqrt{2}} (a_1^\dagger a_3^\dagger \pm a_2^\dagger a_4^\dagger) |0\rangle, \quad (6)$$

$$|\Psi^\pm\rangle = \frac{1}{\sqrt{2}} (a_1^\dagger a_4^\dagger \pm a_2^\dagger a_3^\dagger) |0\rangle. \quad (7)$$

Let $B_\beta(a_1^\dagger, \dots, a_4^\dagger)$, $\beta = 1, \dots, 4$ be the polynomial associated with the above states; the generic input to the network is then represented by the polynomial

$$(P_{\text{in}})_\beta = B_\beta(a_1^\dagger, \dots, a_4^\dagger) Q(a_5^\dagger, \dots, a_n^\dagger), \quad (8)$$

where Q describes the ancillary state $|\Upsilon\rangle$.

At the output of the network, an array of polarizing beamsplitters followed by photon number resolving detectors (PNRD) carries out a measurement in the computational basis. A *detection event* is described by the

number of photons detected in each output mode, *e.g.* 1020 is the event in which three photons are detected, one in the first mode and two in the third mode. This event corresponds to the output state

$$|1020\rangle_{\text{out}} = \frac{c_1^\dagger c_3^{\dagger 2}}{\sqrt{1!0!2!0!}} |0\rangle = \frac{c_1^\dagger c_3^{\dagger 2}}{\sqrt{2}} |0\rangle, \quad (9)$$

and its probability can therefore be computed from the squared norm of the corresponding monomial coefficient in the polynomial (8).

A Bell measurement is *unambiguous* when at least one output event occurs with nonzero probability for only one of the four input Bell states (plus ancilla); events meeting this condition are said to be *discriminating*. By writing p_β^e for the square modulus of the amplitude associated with the detection event e when the input is the Bell state β , the total probability of successful discrimination is:

$$\mathcal{P}_{\text{succ}} = \frac{1}{4} \sum_{e, \tilde{\beta} \in S} p_{\tilde{\beta}}^e \quad \text{with } S = \{e, \tilde{\beta} : \forall \beta \neq \tilde{\beta}, p_\beta^e = 0\}. \quad (10)$$

B. Symbolic computation

The purpose of the method presented here is to provide the optimum-finding algorithm described in the next subsection with a fast, optimized function returning all the detection event probabilities, along with their gradients with respect to the entries of U , from which a figure of merit $f(U)$ will be constructed. Working on this separately, instead of directly using sums of permanents of submatrices of U [26], enables us to carefully analyze the problem and implement some analytical shortcuts that will ultimately speed up the search for optima.

We use SymPy [27], an open-source symbolic computation library for Python. The main procedure is as follows: given an input polynomial in the form (8), we implement the transformation (5) by direct substitution. We then re-group the resulting multivariate polynomial in $c_1^\dagger, \dots, c_n^\dagger$ and we extract the coefficient of each monomial; they correspond to the amplitudes of all possible detection events, and they are complex functions of the entries of U . A straightforward combinatorial argument shows that there are

$$N = \binom{n+k+1}{k+2} \quad (11)$$

possible detection events for each input state, where k is the number of photons in the ancillary state—making $k+2$ the total number of photons entering the network. In the following, we will always assume $n \geq k+4$.

As a simple example of what the algorithm does, consider a network with $n=4$ modes, with the Bell state $|\Phi^+\rangle = B_1|0\rangle$ as input state and no ancillary state ($k=0$), with

$$B_1 = \frac{1}{\sqrt{2}}(a_1^\dagger a_3^\dagger + a_2^\dagger a_4^\dagger).$$

Let U be the unitary matrix representing the network, the output polynomial is obtained upon performing the substitution in eq. (5):

$$P_{\text{out}} = \frac{1}{\sqrt{2}} \left(\sum_{j_1} u_{1j_1} c_{j_1}^\dagger \right) \left(\sum_{j_2} u_{3j_2} c_{j_2}^\dagger \right) + \frac{1}{\sqrt{2}} \left(\sum_{j_3} u_{2j_3} c_{j_3}^\dagger \right) \left(\sum_{j_4} u_{4j_4} c_{j_4}^\dagger \right). \quad (12)$$

After expanding all the products, we obtain a polynomial in $c_1^\dagger, \dots, c_4^\dagger$ with $N=10$ terms of degree $k+2=2$. The coefficient of the monomial $c_1^\dagger c_3^{\dagger 2}$ is, for example, the amplitude of the detection event 1010. For an arbitrary event, with k_i photons in mode i , a bosonic correction factor $\sqrt{\prod_i k_i!}$ has to be applied, as in eq. (9). Expanding (12), all the output event amplitudes read:

$$\begin{aligned} 2000 &\longrightarrow u_{11}u_{31} + u_{21}u_{41} \\ 0200 &\longrightarrow u_{12}u_{32} + u_{22}u_{42} \\ 0020 &\longrightarrow u_{13}u_{33} + u_{23}u_{43} \\ 0002 &\longrightarrow u_{14}u_{34} + u_{24}u_{44} \\ 1100 &\longrightarrow (u_{11}u_{32} + u_{12}u_{31} + u_{21}u_{42} + u_{22}u_{41})/\sqrt{2} \\ 1010 &\longrightarrow (u_{11}u_{33} + u_{13}u_{31} + u_{21}u_{43} + u_{23}u_{41})/\sqrt{2} \\ 1001 &\longrightarrow (u_{11}u_{34} + u_{14}u_{31} + u_{21}u_{44} + u_{24}u_{41})/\sqrt{2} \\ 0110 &\longrightarrow (u_{12}u_{33} + u_{13}u_{32} + u_{22}u_{43} + u_{23}u_{42})/\sqrt{2} \\ 0101 &\longrightarrow (u_{12}u_{34} + u_{14}u_{32} + u_{22}u_{44} + u_{24}u_{42})/\sqrt{2} \\ 0011 &\longrightarrow (u_{13}u_{34} + u_{14}u_{33} + u_{23}u_{44} + u_{24}u_{43})/\sqrt{2}. \end{aligned}$$

The probabilities p_β^e are then obtained by taking the square moduli of those amplitudes. All the above steps are automated in our program, by exploiting polynomial manipulation routines contained in SymPy; we just have to ‘manually’ feed as input the ancillary polynomial Q .

The numerical optimization routine also needs the Jacobian of the figure of merit, and the above approach allows us to compute it symbolically in order to speed up the optimization. This computation is done through the symbolic derivatives of p_β^e with respect to the real and the imaginary part of u_{ij} . The p_β^e are the square modulus of a complex holomorphic function (more precisely, a polynomial) and, for any such function $g(u_{11}, \dots, u_{nn})$, we have

$$\frac{\partial |g|^2}{\partial \text{Re}\{u_{ij}\}} = 2 \text{Re} \left\{ g \frac{\partial g^*}{\partial u_{ij}} \right\}$$

and an analogous expression for the derivative with respect to the imaginary part. This allows for a simple symbolic computation of the relevant derivatives. If the optimization algorithm were not provided with a Jacobian function, it would have had to estimate it by evaluating the figure of merit at nearby points. Using the finite differences method, this amounts to at least $2n^2$ additional evaluations of $f(U)$ per iteration—to be compared

with evaluating n^2 symbolic derivatives, each of which is a strictly simpler function (*i.e.* a polynomial with less terms) than the corresponding probability amplitude. Furthermore the Jacobian would only be calculated to some fixed accuracy, which adds noise to the optimization algorithm and worsen its convergence.

As the output of this computation, we need $4N$ expressions for the probabilities, each one with n^2 expressions for the derivatives. But there is no need to actually compute the symbolic form of all the $4N$ events for each ancilla. Two main simplifications help to drastically reduce the number of symbolic computations:

1. The detection events divide into equivalence classes under permutation of the output modes, corresponding to a permutation of the columns of U . It is easy to check that, of all the events in the above example, it is only necessary to obtain 2000 and 1100. For example, 1010 can be obtained from 1100 by swapping the second and the third column of U , at a negligible computational cost. The number of independent events does not depend on n and is equal to P_{k+2} , the number of integer partitions¹ [28] of the total number of photons. This also reduces the number of gradients to calculate, from n^2 to at most $n(k+2)$.
2. As it is clear from eqs. (6) and (7), knowing an event's amplitudes for a single Bell state allows one to compute its amplitudes for all of them, just by swapping two rows of U and/or changing their sign. This reduces the number of functions to compute by a further factor of 4.

With these expedients, we reduce the problem to the computation of just P_{k+2} probability functions along with their gradients. For example, when $n = 8$, $k = 2$ as in the first scheme of Grice's paper (using a $|\Phi^+\rangle$ ancillary state), we end up decreasing the number of function to compute from $4N = 1320$ to only $P_4 = 5$, each with at most 32 derivatives instead of 64.

As SymPy is written in pure Python, we can accelerate this section of the program using PyPy [29], an implementation of the Python interpreter with a Just-In-Time compiler. For large networks ($n \geq 8$, $k \geq 2$) we obtain a tenfold speedup over plain Python, at the cost of increased memory usage². Even with all these optimizations in place, however, the problem still scales exponentially³. For comparison, we obtain the functions for the first Grice iteration ("one extra Bell pair" in Table II) in about 6

TABLE I. Specifications of the two computers used in this article. The frequency is the nominal frequency of the processor. The cluster is the `gmpcs-206` branch of the computing center MésolUM of the LUMAT research federation [32], and the specifications refer to a single node.

Name	Processor model	# of cores	Freq. (GHz)	RAM (GB)
Laptop	Intel Core i7-4710MQ	4	2.5	16
Cluster	Intel Xeon E5-2670	12	2.3	256

seconds using 100 MB of RAM; the second iteration of Grice's scheme—the largest calculation we managed to complete, with $n = 16$ and $k = 6$ —took instead 10 days of single-core CPU time on the cluster described in Table I, requiring a large portion of the 256 GB of RAM at our disposal. The resulting (already heavily optimized) probability functions for this case consist of a grand total of about 1.8 *million* addition and multiplication operations, and the Jacobian of about 17 million.

We use Theano [31], a numerical computation library for Python, as our backend in order to translate each function into C and compile it to a fast numerical version.

C. Numerical optimization

The second part of the procedure takes care of finding the optimal value of $\mathcal{P}_{\text{succ}}$ in eq. (10) for each input ancillary state. Naively, we could straightforwardly calculate $\mathcal{P}_{\text{succ}}(U)$ from the numerical evaluation of the probability functions obtained in the previous section; however, $\mathcal{P}_{\text{succ}}(U) = 0$ almost everywhere in the domain $U(n)$, and it is neither continuous nor differentiable in the region of interest, where $\mathcal{P}_{\text{succ}}(U) \neq 0$. This obviously makes most optimization methods highly ineffective.

As a workaround, we devise a figure of merit as a continuous alternative to $\mathcal{P}_{\text{succ}}(U)$. We thus search for local *minima* of:

$$f(U) = \sum_e \left(\sum_{\beta} p_{\beta}^e - 2 \max_{\alpha} p_{\alpha}^e \right), \quad (13)$$

of which the addends of the outer sum are equal to the ones of $-\mathcal{P}_{\text{succ}}(U)$, when the latter happen to be nonzero. Ideally, we want the figure of merit to closely mimic the

¹ *I.e.* the number of positive integer sums equal to $k+2$.

² As an example, first iteration of the Ewert-van Loock scheme $(|1\rangle^{\otimes 4} = |\Upsilon_1\rangle_{\text{EVL}}^{\otimes 2})$ takes 7 minutes and 30 seconds on our laptop (see Table I) using the standard Python interpreter and about 150 MB of RAM. Using PyPy the time is cut down to 45 seconds, with a memory consumption of 250 MB.

³ We nonetheless get an exponential advantage over the naive approach, as we can see from the asymptotic formula for P_k due

to Hardy and Ramanujan [30]:

$$P_k \underset{k \rightarrow \infty}{\sim} \frac{1}{4k\sqrt{3}} \exp\left\{ \pi \sqrt{\frac{2k}{3}} \right\},$$

to be compared with the binomial coefficient in eq. (11), lower bounded by 2^{k+2} .

behavior of $\mathcal{P}_{\text{succ}}$ around the optima. In particular it would be useful to have the following holding for each pair of locally optimal unitaries U_1 and U_2 :

$$f(U_1) < f(U_2) \quad \text{iff} \quad \mathcal{P}_{\text{succ}}(U_1) > \mathcal{P}_{\text{succ}}(U_2).$$

Unfortunately, the mutual relation between $f(U)$ and $\mathcal{P}_{\text{succ}}(U)$ is not simple. While it seems reasonable to conjecture the set of local minima of $f(U)$ to include the set of $\mathcal{P}_{\text{succ}}(U)$'s maxima, we find that, for some U_1 and U_2 :

$$f(U_1) < f(U_2) \quad \text{while} \quad \mathcal{P}_{\text{succ}}(U_1) < \mathcal{P}_{\text{succ}}(U_2). \quad (14)$$

This forces us to conduct a search among all local optima of $f(U)$, rather than taking advantage of global optimization methods like simulated annealing.

The optimization itself is implemented using SciPy's *Sequential Least-Square Programming* (SLSQP) optimization method [33, 34]. As this method supports equality constraints, we represent U through $2n^2$ real variables describing its entries' real and imaginary parts, along with n^2 equations enforcing orthonormality of the rows. In order to improve convergence speed, the method is allowed some leniency on the constraints, in that they only have to be satisfied at the local optimum. In order to ensure uniform sampling of the starting points of each optimization, we choose them by picking a random matrix from the Haar measure on the unitary group $U(n)$. This is accomplished using the QR decomposition method described in [35].

We compared the performance of the constrained method above to the Broyden-Fletcher-Goldfarb-Shanno (BFGS) algorithm [36], a popular unconstrained quasi-Newton method. While the latter uses no constraints and has to work with independent variables⁴, the relation between those and the entries of U is non-trivial and this therefore hinders our ability to input the analytical form of the gradient. Thus the performances are comparable with SLSQP, if not worse in some cases, even if the number of variables is cut by half. Furthermore, the convergence accuracy and precision seems unaffected by the choice of one method over the other.

IV. RESULTS

Below, we work out the analytical upper bound for polarization-preserving interferometers in Section II for the states we used, and we compare them to the numerical results we obtained for generic interferometers.

Some of the optimization results for different input ancillae $|\Upsilon\rangle = Q(a_5^\dagger, \dots, a_n^\dagger)|0\rangle$ are summarized in Table II. For each one of them, we collected the local optima from

⁴ We encoded the n^2 unconstrained degrees of freedom of $U(n)$ into an Hermitian matrix H , using $U(n) = e^{iH}$.

about ten thousand successful iterations of the optimization algorithm. In the table the maximum value achieved for each input is shown; it can be noted that, for the cases already known in the literature, we find the same maximal discrimination probability. Furthermore, we were able to work with other types of ancillae.

A. Vacuum extra modes

By virtue of the Calsamiglia-Lütkenhaus theorem [3], the analytical upper bound of $\mathcal{P}_{\text{succ}} \leq 1/2$ is known to hold for general interferometers, equipped with an ancilla consisting of an unlimited number of extra modes in the vacuum state. We can work out different version of this bound (for photon-number- and polarization-preserving measurements) following the reasoning laid out in Section II, looking at the distinguishability of the states in eq. (1) after a projection onto the basis of the number-of-horizontally-polarized-photons operator. If the ancillary state is the vacuum, or any other state with a fixed number $\bar{\lambda}$ of horizontally polarized photons, $v_{\bar{\lambda}}$ is the only value of λ for which $v_{\lambda} \neq 0$. This leads to just two distinct terms:

$$|HH\rangle|\Upsilon\rangle \quad \text{for both } |\Phi^+\rangle \text{ and } |\Phi^-\rangle, \quad (15)$$

$$\pm |VV\rangle|\Upsilon\rangle \quad \text{respectively for } |\Phi^+\rangle, |\Phi^-\rangle. \quad (16)$$

The term (15) is identical for both inputs, while the (16) differs by a global phase. Thus, these terms are not distinguishable at all: in this case the ancillary state cannot help to discriminate between the two different inputs, and $\mathcal{P}_{\text{succ}} \leq 1/2$.

Indeed, without extra photons the maximum discrimination probability that we find through our numerical optimization is 1/2, for any value of n we tried. We quickly achieve this maximum on our laptop (see Table I), and we collect a thousand successful iterations in a matter of minutes for different values of $n \leq 14$. The $n = 14$ case still takes less than an hour on the laptop, and a few minutes of the cluster.

B. Extra Bell pairs

One of the simplest linear optical network schemes with ancilla achieving more-than- $\frac{1}{2}$ Bell state discrimination probability is arguably the first iteration of Grice's strategy [1]. He shows that adding one extra $|\Phi^+\rangle$ as ancilla helps cutting the degeneracy of $|\Phi^\pm\rangle$ by half, achieving $\mathcal{P}_{\text{succ}} = 3/4$. However, the states used by Grice to increase its success probability past 3/4 become more complex at each iteration, since each additional ancillary state $|\Upsilon_N\rangle_G$ is a 2^N -photon GHZ state. It would be experimentally much simpler to use multiple Bell pairs $|\Phi^+\rangle^{\otimes k/2}$ as a k -photon ancilla, which motivate our research of schemes using such resources.

TABLE II. Summary of known analytical and numerical results for different ancillae. Q is the input polynomial, n the number of modes and k the number of photons. $\mathcal{P}_{\text{succ}}^{\text{num}}$ is the optimum obtained through our optical network optimizer; the fraction given is exact up to our numerical precision (9 decimals). $\mathcal{P}_{\text{succ}}^{\text{ana}}$ is the best known explicit analytical result. $\mathcal{P}_{\text{succ}}^{\text{upp}}$ and $\mathcal{P}_{\text{succ}}^{\text{upp}}(k)$ are our analytical upper bounds for polarization-preserving networks (section II), for the ancilla and for arbitrary ancillae with same k . They are in bold font when matching the best known result.

State	Q	n	k	$\mathcal{P}_{\text{succ}}^{\text{num}}$	$\mathcal{P}_{\text{succ}}^{\text{ana}}$	$\mathcal{P}_{\text{succ}}^{\text{upp}}$	$\mathcal{P}_{\text{succ}}^{\text{upp}}(k)$
Vacuum Ancilla							
$ 0\rangle$	1	4–14	0	1/2	1/2[3]	1/2^a[3]	1/2
$k/2$ Extra Bell Pairs							
$ \Phi^+\rangle^{\otimes k/2}$	$\frac{(a_5^\dagger a_7^\dagger + a_6^\dagger a_8^\dagger) \dots (a_{2k+1}^\dagger a_{2k+3}^\dagger + a_{2k+2}^\dagger a_{2k+4}^\dagger)}{2^{k/4}}$	$2k+4$	even	—	b	$1 - \frac{\binom{k/2}{\lfloor k/4 \rfloor}}{2^{k/2+1}}$ ^c $\simeq 1 - \frac{1}{\sqrt{\pi k}}$	$\frac{k+1}{k+2}$
$ \Phi^+\rangle = \Upsilon_1\rangle_G$	$\frac{(a_5^\dagger a_7^\dagger + a_6^\dagger a_8^\dagger)}{\sqrt{2}}$	8	2	3/4	3/4[1]	3/4	3/4
$ \Phi^+\rangle^{\otimes 2}$	$\frac{(a_5^\dagger a_7^\dagger + a_6^\dagger a_8^\dagger)(a_9^\dagger a_{11}^\dagger + a_{10}^\dagger a_{12}^\dagger)}{2}$	12	4	3/4	d	3/4	5/6
$ \Phi^+\rangle^{\otimes 3}$	$\frac{(a_5^\dagger a_7^\dagger + a_6^\dagger a_8^\dagger) \dots (a_{13}^\dagger a_{15}^\dagger + a_{14}^\dagger a_{16}^\dagger)}{\sqrt{8}}$	16	6	e	d	13/16	7/8
k Extra Photons							
$ 1\rangle^{\otimes k}$	$a_5^\dagger \dots a_{k+4}^\dagger$	$k+4$	even	—	b	$1 - \frac{\binom{k/2}{\lfloor k/4 \rfloor}}{2^{k/2+1}}$ ^c $\simeq 1 - \frac{1}{\sqrt{\pi k}}$	$\frac{k+1}{k+2}$
$ 1\rangle^{\otimes k}$	$a_5^\dagger \dots a_{k+4}^\dagger$	$k+4$	odd	—	b	same as above, for $k-1$	
$ 1\rangle$	a_5^\dagger	5	1	1/2 ^d	d	1/2	1/2
$ 1\rangle^{\otimes 2}$	$a_5^\dagger a_6^\dagger$	6	2	5/8	5/8	3/4 ^c (5/8) ^f	3/4
$ 1\rangle^{\otimes 3}$	$a_5^\dagger a_6^\dagger a_7^\dagger$	7	3	5/8	d	3/4 ^c (5/8) ^f	3/4
$ 1\rangle^{\otimes 4} = \Upsilon_1\rangle_{\text{EvL}}^{\otimes 2}$	$a_5^\dagger a_6^\dagger a_7^\dagger a_8^\dagger$	8	4	3/4	3/4[2]	3/4^c	5/6
$ 1\rangle^{\otimes 6}$	$a_5^\dagger \dots a_{10}^\dagger$	10	6	3/4	d	13/16 ^c	7/8
$ 1\rangle^{\otimes 8}$	$a_5^\dagger \dots a_{12}^\dagger$	12	8	e	49/64	13/16 ^c (25/32) ^f	9/10
$ 1\rangle^{\otimes 12}$	$a_5^\dagger \dots a_{16}^\dagger$	16	12	e	25/32[2]	27/32 ^c (13/16) ^f	13/14
Grice Schemes [1] (first iteration is $\Phi^+\rangle = \Upsilon_1\rangle_G$ above)							
$ \Upsilon_1\rangle_G \dots \Upsilon_N\rangle_G$	Straightforward, but long expression	$2k+4$	$2^{N+1}-2$	—	$\frac{k+1}{k+2}$	$\frac{k+1}{k+2}$	$\frac{k+1}{k+2}$
$ \Upsilon_1\rangle_G \Upsilon_2\rangle_G$	$\frac{(a_5^\dagger a_7^\dagger + a_6^\dagger a_8^\dagger)(a_9^\dagger a_{11}^\dagger a_{13}^\dagger a_{15}^\dagger + a_{10}^\dagger a_{12}^\dagger a_{14}^\dagger a_{16}^\dagger)}{2}$	16	6	9/16 ^{gh}	7/8	7/8	7/8
Ewert–van Loock Schemes [2] (first iteration is $1\rangle^{\otimes 4} = \Upsilon_1\rangle_{\text{EvL}}^{\otimes 2}$ above)							
$(\Upsilon_1\rangle_{\text{EvL}} \dots \Upsilon_N\rangle_{\text{EvL}})^{\otimes 2}$	Straightforward, but long expression	$k+4$	$2^{N+2}-4$	—	$\frac{k+2}{k+4}$	$\frac{k+2}{k+4}$	$\frac{k+1}{k+2} \left(\frac{k+2}{k+4} \right)^f$
GHZ states							
$ \text{GHZ}_k\rangle$	$\frac{a_5^\dagger \dots a_{2k+3}^\dagger + a_6^\dagger \dots a_{2k+4}^\dagger}{\sqrt{2}}$	$2k+4$	k	—	3/4 ⁱ	3/4^c	$1 - \frac{1}{\lfloor k+1 \rfloor_{\text{even}}}$
$ \text{GHZ}_3\rangle$	$\frac{a_5^\dagger a_7^\dagger a_9^\dagger + a_6^\dagger a_8^\dagger a_{10}^\dagger}{\sqrt{2}}$	10	3	3/4	3/4 ⁱ	3/4^c	3/4
$ \text{GHZ}_4\rangle = \Upsilon_2\rangle_G$	$\frac{a_5^\dagger a_7^\dagger a_9^\dagger a_{11}^\dagger + a_6^\dagger a_8^\dagger a_{10}^\dagger a_{12}^\dagger}{\sqrt{2}}$	12	4	3/4	3/4 ⁱ	3/4^c	5/6
W State							
$ W_3\rangle$	$\frac{a_6^\dagger a_7^\dagger a_9^\dagger + a_5^\dagger a_8^\dagger a_{10}^\dagger + a_5^\dagger a_7^\dagger a_{10}^\dagger}{\sqrt{3}}$	10–11 12–14	3	5/9 ^h 0.5785508(2) ^h	7/12	2/3 ^c (3/4) ^j	3/4

^a Also holds for polarization non-preserving interferometers.

^b No generic scheme is known.

^c Polarization-preserving bound obtained after rotating the polarization of some or all modes by $\frac{\pi}{4}$.

^d The best known interferometer correspond to a smaller ancilla, together with ignoring extra modes.

^e Computation out of reach for our program.

^f For networks which start by interfering the two bell states on a 50:50 beamsplitter, analyzing each half separately.

^g Computation at the borderline of our computing capacity: this result is the best of just 12 optimizations over the course of three weeks.

^h Numerical result worse than the best known analytical scheme.

ⁱ Success probability achieved by measuring all photons of the ancilla and using the remaining in a “one extra Bell pair” scheme.

^j Obtained through a more complex transformation of the input, exposed in the main text.

We start by working out the polarization-preserving bound of Section II. We restrict ourselves to a product of $k/2$ states of the form $|\Upsilon_1\rangle = \frac{1}{\sqrt{2}}(|2H\rangle + |2V\rangle)$, where $|2H\rangle$ (resp. $|2V\rangle$) is any state of two horizontally (resp. vertically) polarized photons. Bell pairs are a special case of the latter, as well as the $|\Upsilon_1\rangle_{\text{EvL}}$ defined in [2]. We have

$$\begin{aligned} |\Upsilon_1\rangle^{\otimes k/2} &= 2^{-k/4}(|2H\rangle + |2V\rangle)^{\otimes k/2} \\ &= 2^{-k/4} \sum_{\lambda=0}^{k/2} \sqrt{\binom{k/2}{\lambda}} |\Upsilon, 2\lambda\rangle, \end{aligned}$$

where $|\Upsilon, 2\lambda\rangle$ is the uniform superposition of the terms with 2λ horizontally polarized photons present in the expansion of $|\Upsilon_1\rangle^{\otimes k/2}$. Equation (2) then only have even nonzero terms, and this leads to

$$\mathcal{P}_{\text{fail}}^{\substack{\text{fail} \\ |\Phi^+\rangle^{\otimes k/2}}} \geq 2^{-k/2-1} \binom{k/2}{\lfloor k/4 \rfloor} \quad (17)$$

$$\begin{aligned} &\geq 2^{-k/2-1} \frac{1}{\sqrt{\pi k}} 2^{k/2+1} e^{-2/3k} \\ &= \frac{1}{\sqrt{\pi k}} e^{-2/3k}, \end{aligned} \quad (18)$$

where we have supposed k to be a multiple of 4 and applied a second-order version of Stirling's approximation [37]

$$\sqrt{2\pi n} \left(\frac{n}{e}\right)^n \leq n! \leq \sqrt{2\pi n} \left(\frac{n}{e}\right)^n e^{1/12n}$$

When k is even, but not a multiple of 4, the inequality (18) is invalid, but we still have

$$\mathcal{P}_{\text{fail}}^{\substack{\text{fail} \\ |\Phi^+\rangle^{\otimes k/2}}} \geq \frac{1}{\sqrt{\pi k}} \left(1 + O\left(\frac{1}{k}\right)\right). \quad (19)$$

The $1/\sqrt{k}$ scaling of $\mathcal{P}_{\text{fail}}$ allowed by the above bound is worse than the $1/k$ scaling achieved by Grice schemes. Nevertheless, it does not rule out strategies approaching success probabilities arbitrarily close to 1 by using as inputs much simpler states, *i.e.* $k/2$ Bell pairs.

Our numerical search, which is not restricted to polarization-preserving schemes, converges in just about a minute to the $\mathcal{P}_{\text{succ}} = 3/4$ scheme on our laptop, using 300 MB of RAM. Unfortunately, the use of two extra Bell pairs shows no improvement over a single extra Bell pair, and its optimization uses significantly more resources: about 4 hours with 20 parallel threads on the cluster (see Table I), each using 3 GB of RAM, for the collection of a thousand optimizations. For three extra-bell pairs, the polarization-preserving bound of eq. (17) gives $\mathcal{P}_{\text{succ}} \leq 13/16 = .8125$ for the latter, allowing in principle for a scheme beyond $3/4$. However, this dimensionality is barely out of reach for our program, even using the cluster. For comparison with a similar-sized case, the second iteration of Grice's strategy (the symbolic function's sheer size of which we discussed at the end of Section III B)

takes about 48 hours on the cluster for each starting point to converge to a local optimum. We collected just 12 optimizations, obtaining $\mathcal{P}_{\text{succ}} = 9/16$; unfortunately this result is well below the known Grice's $7/8$ scheme.

C. Extra single photons

The possibility of improving the discrimination probability through the use of unentangled extra single photons is of great experimental interest, especially with the recent development of high-efficiency single photon sources with near ideal indistinguishability [38]: such ancillary states would be among the simplest types of input states for a real-world implementation of linear optical Bell measurements.

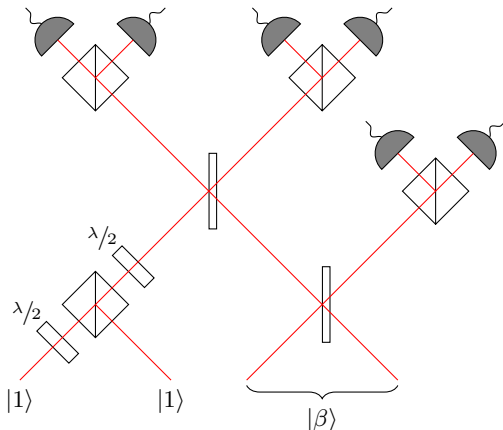
Ewert and van Loock explore the use of pairs of single photon per auxiliary dual-rail mode [2, Section D of supp. mat.] as substitutes of their ancillary state $|\Upsilon_1\rangle_{\text{EvL}}$. While the initial transformation they apply to the input photons is polarization dependent, we can still use the formalism of our polarization-preserving upper bound of Section II, restricted to the case in which each photon enters the network polarized along the $\pm\frac{\pi}{4}$ direction. In the horizontal-vertical basis, this ancilla is described by the Hong-Ou-Mandel state [39] $|\Upsilon_1\rangle_{\text{EvL}} = \frac{1}{\sqrt{2}}(|20\rangle + |02\rangle)$ in each mode pair. The v_λ coefficients in the case of the k -photon state (with k even) $|\Upsilon_1\rangle_{\text{EvL}}^{\otimes k/2}$ correspond to the ones of $k/2$ Bell states $|\Phi^+\rangle^{\otimes k/2}$. We can therefore apply the same reasoning laid out in Section IV B, obtaining the bound in eq. (17).

With this restriction in place, we get for $k \geq 4$ a slightly tighter lower bound to $\mathcal{P}_{\text{fail}}$, compared to the photon-number based bound (4). For example, with 4 single photons the latter gives $\mathcal{P}_{\text{fail}} \geq 1/6$, while eq. (17) gives $\mathcal{P}_{\text{fail}} \geq 2^{-3} \binom{2}{1} = 1/4$. In fact, the bound is saturated by the 4-single-photon variant of the first iteration of Ewert-van Loock strategy. They also consider the 12-single-photon state $|1\rangle^{\otimes 12} \rightarrow |\Upsilon_1\rangle^{\otimes 6}$. In this case, a direct application of equation (17) leads to $\mathcal{P}_{\text{fail}} \geq 2^{-7} \binom{6}{3} = 5/32$, which is indeed smaller than the actual $7/32$ failure rate found by the authors. However a look into the detailed symmetry of the strategy, as per the same reasoning used at the end of Section II B, leads to the better (but more restricted) bound $\mathcal{P}_{\text{fail}} \geq 2^{-4} \binom{3}{1} = 3/16$, which is closer, but still below $7/32$.

The aforementioned 4-photon scheme discriminates $|\Psi^+\rangle$ and $|\Psi^-\rangle$ with certainty, and $|\Phi^\pm\rangle$ only half of the times. Our numerical algorithm indeed finds this $(1, 1, \frac{1}{2}, \frac{1}{2})$ scheme when initialized with a 4 single photon ancilla, and does not manage to improve its probability of success—an evidence of its optimality even in the polarization-dependent case. Furthermore, we find other schemes achieving the same total success probability with a different discrimination pattern among the Bell states: $(1, \frac{3}{4}, \frac{3}{4}, \frac{1}{2})$.

Interestingly, with just two extra photons, we find two

FIG. 1. The first “half” Ewert–van Loock single-photons scheme. It performs a Bell measurement with $\mathcal{P}_{\text{succ}} = 5/8$ on the state $|\beta\rangle$ using two unentangled extra photons $|1\rangle$, two polarization-independent beamsplitters, four polarizing beamsplitters, two phase shifters and six photodetectors.



schemes, $(1, 1, \frac{1}{4}, \frac{1}{4})$ and $(1, \frac{3}{4}, \frac{1}{2}, \frac{1}{4})$, achieving a discrimination probability of $\mathcal{P}_{\text{succ}} = 5/8 = 0.625$. The first can be easily described as half of the 4-photon Ewert–van Loock scheme [2] mentioned above and is described in Figure 1. It is especially relevant experimentally, since it is the simplest scheme achieving a success rate above $1/2$. It was independently obtained by Ewert and van Loock [40]. By “halving” in the same way the Ewert–van Loock 12-photon scheme that uses $4 + 8$ single photons and achieves a probability of $25/32$, we find a similar “intermediate” scheme with $4+4=8$ extra photons, achieving $\mathcal{P}_{\text{succ}} = 49/64$. Unfortunately, even using the cluster, numerically testing this scheme ($n = 12, k = 8$) proved to be unfeasible.

We notice (as in [19]) that using an odd number $k + 1$ of single photons in the ancilla does not improve the discrimination probability over the case with k photons. This is in line with the analytically-derived behavior for polarization-preserving interferometers of Section II B.

Very recently, Smith and Kaplan [19] tackled a similar problem, numerically optimizing linear optical Bell measurements with single photons ancillæ. Their measurement were allowed to be ambiguous, and the chosen figure of merit was the classical mutual information between state preparation and measurement. Remarkably, despite this difference, we find corresponding results for ancillæ up to five single-photons; with six photons, they find a slight improvement of their mutual information, but the corresponding measurement is ambiguous [41]. Even if with six photons (Table II) we could not find any scheme beyond $\mathcal{P}_{\text{succ}} = 3/4$ —we collected more than 10 000 optimizations—the polarization-preserving bound allows for a scheme with $\mathcal{P}_{\text{succ}} \leq 13/16$; an improvement over $3/4$ is therefore not excluded.

D. GHZ and W states

We also checked the possible use of multipartite entangled states and ancillæ. A three-photon GHZ state ancilla,

$$|\text{GHZ}_3\rangle = \frac{1}{\sqrt{2}}(|000\rangle + |111\rangle),$$

does not seem to help with respect to a simple Bell pair, as we still attain $3/4$ discrimination probability as optimum. So does a GHZ_4 state, at the expense of more computational power; we wrongly expected the latter to be useful, given its use (along with a Bell pair) in the second iteration of Grice’s scheme [1]. The analytical polarization-preserving bound predicts $\mathcal{P}_{\text{succ}} \leq 1/2$ for all $|\text{GHZ}_k\rangle$ when $k \geq 3$. However, for odd k , the rotation of the polarization of a single photon by an angle of $\pm \frac{\pi}{4}$ raises this bound to $3/4$. This value can be achieved by a trivial network applying a simple $\frac{\pi}{4}$ rotation on $k - 2$ spatial modes of the ancilla, which leaves the remaining two photons in the $|\Phi^\pm\rangle$ states, which can be used as described above⁵ to achieve a $3/4$ success probability.

Another interesting state to investigate is the three-photon W state,

$$|W_3\rangle = \frac{1}{\sqrt{3}}(|100\rangle + |010\rangle + |001\rangle). \quad (20)$$

Like GHZ_3 , it is a genuinely 3-party entangled state but, unlike all other states studied above, it is not a graph state, not even a stabilizer state. Its specific symmetry is likely the source of the interesting results we find (end of Table II). Having the same number of horizontally polarized photons in each term, this state is as useful as the vacuum for polarization-preserving interferometers, as showed in Section IV A. However, the rotation of the polarization of two photons by $\frac{\pi}{4}$ gives the higher bound $\mathcal{P}_{\text{succ}} \leq 2/3$, and further manipulation (see below) raises this bound to $\mathcal{P}_{\text{succ}} \leq 3/4$. The best optimum we find numerically, when we use a network with no extra vacuum modes ($n = 10$), is $\mathcal{P}_{\text{succ}} = 5/9$, significantly lower than the $3/4$ achieved with a simpler two-photon Bell pair. This optimum is extremely rare (once in more than 20 000 optimizations), and we observe the figure of merit in this case to suffer heavily from the problem described in eq. (14) about the relationship between $f(U)$ and $\mathcal{P}_{\text{succ}}(U)$.

However, in this case we could find a better scheme by manipulating the state “by hand”. By measuring the last two spatial modes we can apply a transformation such that the remaining modes can be, depending on the result of the measurement, either in the state $\frac{1}{\sqrt{2}}(|2H, 0\rangle - |0, 2V\rangle)$

⁵ The phase of the Bell pair is determined by the parity of the measurement of the $k - 2$ photons, and its effect is simply exchanges the photon patterns for the detection of $|\Phi^+\rangle$ and $|\Phi^-\rangle$.

or $|\Phi^+\rangle$. Applying to these modes the same unitary of the one-Bell-pair $\mathcal{P}_{\text{succ}} = 3/4$ Grice strategy gives a scheme for $|\mathcal{W}_3\rangle$ with $\mathcal{P}_{\text{succ}} = 7/12$. While our optimization program correctly identifies this scheme as a local optimum when put in as starting point, an added Gaussian noise of average magnitude well below the requested convergence accuracy is sufficient for the optimization to diverge from it. This numerical fragility may be the reason why we could not find this optimum through the optimization. Applying the analytical bound to such transformed ancilla gives us $\mathcal{P}_{\text{succ}} \leq 3/4$. Interestingly, adding at least two vacuum modes ($n \geq 12$) allows the program to reach the better discrimination probability of 0.5785508(2). Still, this is slightly below the manually-found 7/12.

V. CONCLUSION

In this work we have investigated the optimal success probability of a linear optical Bell measurement assisted by different kinds of input ancillary states $|\Upsilon\rangle$. In Section II, we showed how to obtain an upper bound from the input photon polarization distribution in $|\Upsilon\rangle$, when the network is restricted to polarization-preserving interferometers; we noticed that the bound is tight for some published schemes. With the aim of exploring the parameter space of generic interferometers, we developed in Section III a linear optical network simulator, capable of evolving a generic input state through the network and computing the analytical expression of the probabilities of each detection event in the output. We then conducted a numerical search for the optimal value of $\mathcal{P}_{\text{succ}}$ in for fixed $|\Upsilon\rangle$, and we discussed how to reduce the overall computational cost by exploiting some symmetries of the problem at hand. We presented the results of both analytical and estimated numerical bounds in Section IV, and we recall them in Table II.

Through both the analytical study and the numerical optimization we find evidences (but no proofs) for the optimality of known small schemes. Some of them seem achievable experimentally in the short term, as they require as ancilla either a small number of photons or an additional Bell pair. While restricted to the polarization-preserving case, the photon-number based analytical upper bound, saturated by Grice's schemes, is evidence for their optimality if resources are measured in terms of the number of extra ancillary photons. In this setting, we

have also shown that employing many copies of a Bell pair leads to a different (and worse) scaling than using Grice's states, giving interesting insights into the reason why the big GHZ-like states that appear in the schemes of [1, 2] are needed. Of course, eq. (17) being only a bound, more research is needed to investigate its tightness, and whether near unity success can indeed be achieved.

As pointed out in the paper, some interesting cases lie beyond the computational capabilities at our disposal. While there is still room for improvement, *e.g.* by further optimization of the code and/or by employing more CPU time, our numerical approach is at least as hard as computing permanents of $k \times k$ submatrices of a unitary matrix. As proved by Valiant [42] and more recently pointed out by Arkhipov and Aaronson [43] in the context of linear optics, this task pertains to the complexity class $\#\text{P-hard}$ and is not believed to be solvable in polynomial time on a classical computer. However the symmetry of the Bell states and the unambiguity constraints, which enforce a structure on the matrix entries—by imposing many null probabilities—may enable significant speedups (even exponential ones), even if the overall scaling could stay exponential. Recent works in [44, Appendix B] and [45, Appendix D] suggest optimized algorithms for computing the permanent of matrices with repeated columns/rows; they may help to improve our computation.

We conclude by noting that our simulator might be useful in exploring the power of linear optics in solving other types of problems. Due to the flexibility of Python and of the separation between symbolic computation and numerical optimization, the program only requires minor modifications in order to be adapted to new tasks. As a matter of fact, it has already been used during discussions with Chabaud *et al.* in order to gain insight on the effect of Hadamard networks, helping in the design of linear optical swap-test [46].

ACKNOWLEDGMENTS

We warmly thank the Quantum Information team of the LIP6 for their hospitality, and especially Ulysse Chabaud for stimulating discussions. We acknowledge the use of the computing center MésoLUM of the LUMAT research federation (FR LUMAT 2764). AO acknowledges financial support from ANR project ANR-16-CE39-0001 and the Erasmus+ Traineeship Programme of the European Union.

[1] W. P. Grice, *Physical Review A* **84**, 042331 (2011).
 [2] F. Ewert and P. van Loock, *Physical Review Letters* **113**, 140403 (2014).
 [3] J. Calsamiglia and N. Lütkenhaus, *Applied Physics B* **72**, 67 (2001).
 [4] S. L. Braunstein and A. Mann, *Physical Review A* **51**, R1727 (1995).

[5] C. H. Bennett, G. Brassard, C. Crépeau, R. Jozsa, A. Peres, and W. K. Wootters, *Physical Review Letters* **70**, 1895 (1993).
 [6] S.-W. Lee and H. Jeong, in *proceedings of the First International Conference on Entangled Coherent State and Its Application to Quantum Information Science* (Tamagawa University, Tokyo, 2012) pp. 41–46.

- [7] D. Bouwmeester, J.-W. Pan, K. Mattle, M. Eibl, H. Weinfurter, and A. Zeilinger, *Nature* **390**, 575 (1997).
- [8] C. H. Bennett and S. J. Wiesner, *Physical Review Letters* **69**, 2881 (1992).
- [9] K. Mattle, H. Weinfurter, P. G. Kwiat, and A. Zeilinger, *Physical Review Letters* **76**, 4656 (1996).
- [10] M. Żukowski, A. Zeilinger, M. A. Horne, and A. K. Ekert, *Physical Review Letters* **71**, 4287 (1993).
- [11] J.-W. Pan, D. Bouwmeester, H. Weinfurter, and A. Zeilinger, *Physical Review Letters* **80**, 3891 (1998).
- [12] N. Lütkenhaus, J. Calsamiglia, and K.-A. Suominen, *Physical Review A* **59**, 3295 (1999).
- [13] E. Knill, R. Laflamme, and G. J. Milburn, *Nature* **409**, 46 (2001).
- [14] P. Kok, W. J. Munro, K. Nemoto, T. C. Ralph, J. P. Dowling, and G. J. Milburn, *Reviews of Modern Physics* **79**, 135 (2007).
- [15] H. A. Zaidi and P. van Loock, *Physical Review Letters* **110**, 260501 (2013).
- [16] D. Vitali, M. Fortunato, and P. Tombesi, *Physical Review Letters* **85**, 445 (2000).
- [17] S.-W. Lee and H. Jeong, *Physical Review A* **87**, 022326 (2013).
- [18] S.-W. Lee, K. Park, T. C. Ralph, and H. Jeong, *Physical Review Letters* **114**, 113603 (2015).
- [19] J. A. Smith and L. Kaplan, [arXiv:1802.10527 \[quant-ph\]](https://arxiv.org/abs/1802.10527) (2018).
- [20] A. Olivo and F. Grosshans, arxiv.org/src/1806.01243/anc (supplementary information of this paper, 2018).
- [21] I. Ivanovic, *Physics Letters A* **123**, 257 (1987).
- [22] D. Dieks, *Physics Letters A* **126**, 303 (1988).
- [23] A. Peres, *Physics Letters A* **128**, 19 (1988).
- [24] D. M. Greenberger, M. A. Horne, and A. Zeilinger, in *Bell's Theorem, Quantum Theory and Conceptions of the Universe* (Springer Netherlands, Dordrecht, 1989) pp. 69–72.
- [25] V. Fock, *Zeitschrift für Physik* **75**, 622 (1932); english translation in L. D. Faddeev, L. A. Khal'fin, and I. V. Komarov, *V.A. Fock-selected works : quantum mechanics and quantum field theory* (Chapman & Hall/CRC, 2004) p. 567.
- [26] S. Scheel, in *Quantum Information Processing* (Wiley-VCH Verlag GmbH & Co. KGaA, Weinheim, FRG, 2005) pp. 382–392.
- [27] A. Meurer, C. P. Smith, M. Paprocki, O. Čertík, S. B. Kirpichev, M. Rocklin, A. Kumar, S. Ivanov, J. K. Moore, S. Singh, T. Rathnayake, S. Vig, B. E. Granger, R. P. Muller, F. Bonazzi, H. Gupta, S. Vats, F. Johansson, F. Pedregosa, M. J. Curry, A. R. Terrel, S. Roučka, A. Saboo, I. Fernando, S. Kulal, R. Cimrman, and A. Scopatz, *PeerJ Computer Science* **3**, 27 (2017).
- [28] M. Abramowitz, I. A. Stegun, and R. H. Romer, *American Journal of Physics* **56**, 958 (1988).
- [29] S. Pedroni, “Goals and Architecture Overview — PyPy documentation,” .
- [30] G. H. Hardy and S. Ramanujan, *Proceedings of the London Mathematical Society* **s2-17**, 75 (1918).
- [31] Theano Development Team, [arXiv:1605.02688 \[cs.SC\]](https://arxiv.org/abs/1605.02688) (2016).
- [32] <http://www.mesolum.lumat.u-psud.fr> (Mésocentre Lumière Matière – MésoLUM).
- [33] T. E. Oliphant, *Computing in Science and Engineering* (2007), 10.1109/MCSE.2007.58.
- [34] D. Kraft, *A software package for sequential quadratic programming*, Forschungsbericht. Deutsche Forschungs- und Versuchsanstalt für Luft- und Raumfahrt, DFVLR (DFVLR, Braunschweig, 1988).
- [35] M. Ozols, “How to generate a random unitary matrix,” (2009).
- [36] J. Nocedal and S. J. Wright, *Numerical optimization* (Springer, 2006) p. 664.
- [37] H. Robbins, *The American Mathematical Monthly* **62**, 26 (1955).
- [38] P. Senellart, G. Solomon, and A. White, *Nature Nanotechnology* **12**, 1026 (2017).
- [39] C. K. Hong, Z. Y. Ou, and L. Mandel, *Physical Review Letters* **59**, 2044 (1987).
- [40] P. van Loock, in *presentation at “Secure Communication via Quantum Channels”* (Bielefeld, Germany, 2017).
- [41] J. A. Smith, private communication (2017).
- [42] L. Valiant, *Theoretical Computer Science* **8**, 189 (1979).
- [43] S. Aaronson and A. Arkhipov, *Theory of Computing* **9**, 143 (2013).
- [44] M. C. Tichy, *Entanglement and interference of identical particles*, *Ph.D. thesis*, Freiburg University (2011).
- [45] V. S. Shchesnovich, *International Journal of Quantum Information* **11**, 1350045 (2013).
- [46] U. Chabaud, E. Diamanti, D. Markham, E. Kashefi, and A. Joux, [arXiv:1805.02546 \[quant-ph\]](https://arxiv.org/abs/1805.02546) (2018).